Electrotransport of proton and divalent cations through modified cation-exchange membranes

Agnès Chapotot, Gérald Pourcelly, Claude Gavach, Frédéric Lebon

Electrotransport of proton and divalent cations through modified cation-exchange membranes

Agnès Chapotot [a], Gérald Pourcelly [a], Claude Gavach [a,*], Frédéric Lebon [b]

[a] *Laboratory of Materials and Membrane Processes, UMR9987, CNRS, BP5051, 34033 Montpellier Cédex, France*
[b] *Laboratory of Mechanics and Civil Engineering, University of Montpellier II, 34095 Montpellier Cédex 5, France*

Separation of divalent cations from binary electrolyte solutions with protons was achieved by electrotransport through modified cation-exchange membranes (CEMs). The CEM modification was carried out by adsorption of polyethylenciminc on the membrane surface. Without any applied driving force, both modified and non-modified membranes exhibited a higher affinity for divalent cations. Under an electrical field, the transport number of the divalent cation decreased significantly. The apparent rate constants of the penetration of the divalent cations into the membrane were calculated on the basis of unidirectional fluxes and concentration profiles of cations within the anodic unstirred layer. The unidirectional fluxes were measured by means of the radiotracer technique. The concentration profiles were determined by numerical resolution of the Nernst–Planck electrodiffusion equations coupled with the Poisson equation for current densities lower than the limiting value.

Keywords: Cation-exchange membranes; Electrotransport; Radiotracers; Unidirectional flux; Kinetics

1. Introduction

Experimental research has been devoted to the development of a new type of cation-exchange membrane (CEM) which can not only separate cations from anions but also separate cations of different valences. This type of CEM has preferential selectivity. These CEMs can improve the performances of existing processes without the addition of surface-active agents or polyelectrolytes in the solution to be treated [1–3].

These CEMs can be used in various applications such as the electrodialysis (ED) of seawater or spent mineral acids or in redox-flow batteries. Indeed, in the case of the sea-water concentration processes to obtain raw salt or edible salt, CEMs with preferential selectivity for monovalent cations can avoid the formation of scales (e.g. $CaCO_3$, $CaSO_4$ etc.) which can form in the concentration chambers [4,5].

Waste acids containing metallic salts are produced by several industries, such as pickling and surface treatment, the pigment industry and hydrometallurgy. Nowadays, these industries trend to treat these effluents in order to re-use and recycle pollutants and to conserve raw materials. CEMs with preferential selectivity for monovalent cations would make the ED process competitive with traditional processes. Moreover, the existing treatment of acid wastes is now controversial for environmental reasons because diluted effluents are dumped into rivers or the sea, and sludge is deposited in dumps.

The synthesis of CEMs with preferential selectivity for monovalent cations would also enable the commercial production of redox-flow batteries. This kind of battery is of great interest to NASA and in Japan, where it is a theme of the "Moon-Light" project of the Ministry of International Trade and Industry [6].

A CEM can be made preferentially selective to monovalent cations by depositing a thin anion exchange layer on its surface [7]. The positive charges introduced on the surface create an electrostatic repulsion which is greater for multivalent cations than for monovalent cations [8,9]. The method that we have

* Corresponding author.

selected for obtaining a CEM with preferential permselectivity for monovalent cations consists in immersing the CEM in an aqueous solution of polyelectrolyte which is adsorbed on the membrane surface. The method has been described previously by Sata [10]. Furthermore, this allows the use of a commercial CEM and a reference CEM; it is also a very convenient method which gives a surface film that is sufficiently stable for our experiments.

The aim of this work is to obtain a better understanding of the mechanism of preferential selectivity of modified CEM to protons. We describe the properties of a modified CEM both under equilibrium conditions and when it functions in an electrical field.

2. Experimental

The commercial cation-exchange membrane used in this study was a CRA membrane obtained from Solvay Co. It was composed of a poly(ethylene-tetrafluoroethylene) copolymer (ETFE) matrix cross-linked with divinylbenzene and bearing sulphonic ion-exchange groups. This membrane has been specially designed for the treatment of effluents from metal pickling. Before measurements, the CRA membrane was equilibrated in the electrolyte solution for at least 24 h.

2.1. Surface modification

The surface of the CRA membrane was modified by adsorption or ion exchange of the polyelectrolyte polyethyleneimine (PEI) which was obtained from Fluka Chemika Co. PEI has a molar mass between 6×10^5 and 10^6 g. The membrane sample (area 25 cm^2) was placed in a 0.1 M aqueous HCl solution to equilibrate the sulphonic exchange sites with protons, after which it was immersed in a stirred PEI aqueous solution of given concentration at room temperature for 48 h. The concentration of PEI in the treatment solution was in the range 5–4000 ppm. The sample was then equilibrated with the electrolyte solution. We use the following nomenclature to define the modified membranes: the CRA membrane whose surface was modified in an aqueous solution containing X ppm of PEI is designated CRA-X.

The amount of adsorbed PEI was measured by determining the polyelectrolyte concentration before and after the immersion cycle. This concentration was analysed using the UV absorption spectrum of the copper–PEI complex [10]. To do this, the solution containing PEI was mixed with a cupric sulphate solution. The maximum absorption of the copper–PEI complex was located at 275 μm. Electron spectroscopy allows the determination of the thickness of the modified layer, which is estimated to be less than 1 μm.

2.2. Exchange capacity, water content and ion exchange isotherms

The techniques used to determine the exchange capacity, the water content and the ion-exchange isotherms have been described extensively in previous papers [11,12].

2.3. Electrical resistance and current–voltage measurements

The electrical resistance was measured using the clip-cell described elsewhere [12]. The frequency of the applied current was 1000 Hz. The current–transmembrane potential difference curves for obtaining the values of the limiting current were recorded using the apparatus described previously by Taky et al. [13].

2.4. Preferential selectivity

The selectivity of the modified membranes towards Ca^{2+} with respect to protons and their selectivity towards chloride ions were quantified as the relative transport number of these ions under a constant current. The transport numbers were measured by means of radiotracers. Radiotracer measurements allow the determination of the unidirectional fluxes of ions according to a technique described elsewhere [14]. ^{45}Ca-labelled $CaCl_2$ for the Ca^{2+}–H^+ selectivity and ^{36}Cl-labelled NaCl for the selectivity towards chloride ions were obtained from Amersham Radiochemical Centre. Current–voltage responses and radiotracer measurements were carried out under identical concentrations on both sides of the membrane (symmetrical conditions) and under constant hydrodynamic conditions. The principle of the measurements is illustrated in Fig. 1(a) for the determination of calcium flux.

The Ni^{2+}–H^+ selectivity was achieved using Hittorf's method in the asymmetric electro-electrodialysis cell shown in Fig. 1(b). The anode compartment contained 200 ml of a mixed solution (0.5 M H_2SO_4 + 0.5 M $NiSO_4$) while the cathode compartment contained only 50 ml of a 1 M H_2SO_4 solution. The low volume of the cathode compartment facilitated detection of the concentration variations, while the larger volume of the anode compartment enabled this variation to be minimized. The active surface area of the membrane was 7 cm^2 and the applied current density was 30 mA cm^{-2}.

The selectivity of the modified membranes towards sulphate ions was measured using the same asymmetric cell. In this case, the anode compartment was filled with 20 ml of a 0.05 M H_2SO_4 solution and the cathode compartment contained 200 ml of a 2 M H_2SO_4 solution in order to provide favourable conditions for sulphate leakage. The applied current density was 50 mA cm^{-2}.

3. Results

3.1. Main characteristics of the modified membranes

The amount of PEI adsorbed on the CRA membrane was a linear function of the PEI concentration of the treatment solution (about 0.11 mg cm^{-2} PEI for 1000 ppm of PEI in the treatment solution). Therefore the amount of PEI adsorbed was very low. It could not be detected by X-ray photoelectron spectroscopy (XPS) analysis. Electron spectroscopy showed that the surface aspects of modified CRA-1000 and non-modified CRA membrane were similar. However, because the surface film was torn on a CRA-1000 sample, its thickness could only be estimated as being of the order of 10^{-2} μm.

The exchange capacities of the modified and non-modified membranes did not vary significantly ranging from 2.14 to 2.16 mmol g^{-1} of dried membrane in the Na^+ form on going from the CRA to the CRA-1000 membrane). Similarly, the surface modification did not modify the water content, defined as the ratio of the amount of water inside the membrane to the mass of dried membrane (38%–39%). Consequently, it can be concluded that neither the exchange capacity not the water content are affected by surface modification.

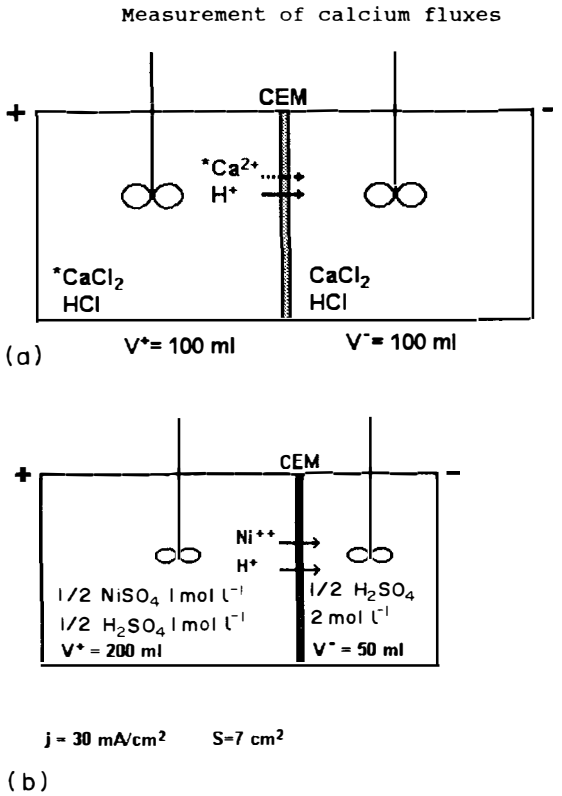

Fig. 1. Experimental cells: (a) determination of calcium flux by the radiotracer technique; (b) determination of the Ni^{2+} transport number using Hittorf's method.

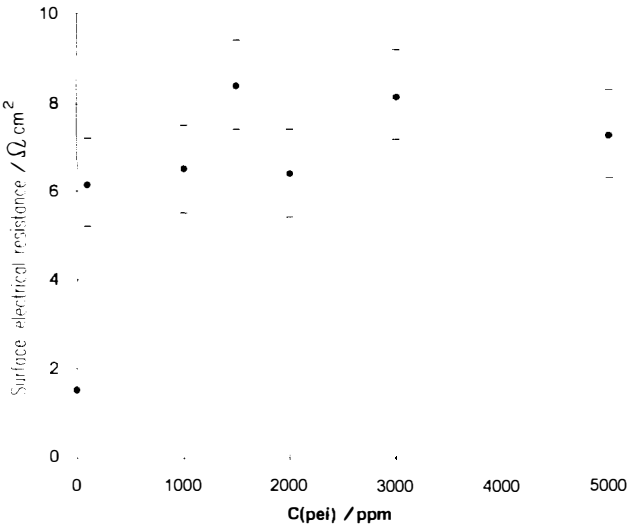

Fig. 2. Surface electrical resistance vs. concentration of PEI in the immersion solution.

3.2. Electrical resistance

The presence of a polyelectrolyte film at the surface of the CRA membrane increases its electrical resistance. A balance has to be found between this increase, which enhances the transmembrane potential difference, and the increase of the selectivity towards monovalent cations with respect to divalent cations. As shown in Fig. 2, when the modified CRA membranes are equilibrated in a 0.17 M NaCl solution, the values of their surface electrical resistances as a function of the PEI concentration in the treatment solution increase from 1.6 Ω cm^2 for the non-modified CRA membrane to a maximum value of 7–8 Ω cm^2 for PEI concentrations greater than 2000 ppm.

When the modified CRA membranes were equilibrated with a mixed solution of $CaCl_2$ + HCl, with a total charge equivalent concentration of 0.1 M, a decrease in the surface resistance with the molar fraction of proton inside the membrane was observed (Fig. 3). As with the membranes equilibrated with the 0.17 M NaCl solution, the increase in the PEI concentration in the treatment solution increases the electrical resistance of the modified membranes. However, the electrical resistance reaches a constant value when the PEI concentration of the immersion solution exceeds 100 ppm.

3.3. Ion-exchange isotherms

Ion-exchange isotherms between Ca^{2+} ions and protons were determined using a technique described in detail elsewhere [11]. Fig. 4 shows that the ion-exchange isotherms are not significantly different for the modified membranes. Therefore the presence of the

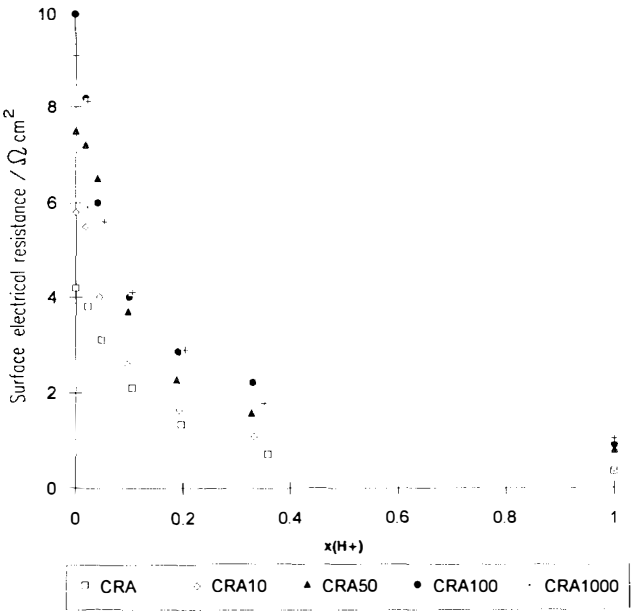

Fig. 3. Surface electrical resistance vs. equivalent ionic fraction of protons in the membrane.

surface film of PEI does not affect the preference of the CRA membrane for divalent ions.

3.4. Current–voltage measurements

Current–voltage curves were recorded for the non-modified CRA membrane and for the modified CRA-5 and CRA-1000 membranes for different $Ca^{2+} + H^+$ contents in the equilibrating solutions ($\frac{1}{2}CaCl_2 + HCl$: 0.075 + 0.025, 0.05 + 0.05 and 0.025 + 0.075 mol l^{-1}). In the field of applied current densities, from zero to 40 mA cm^{-2}, the limiting current density was never reached. The hydrodynamic conditions were kept constant during all the experiments.

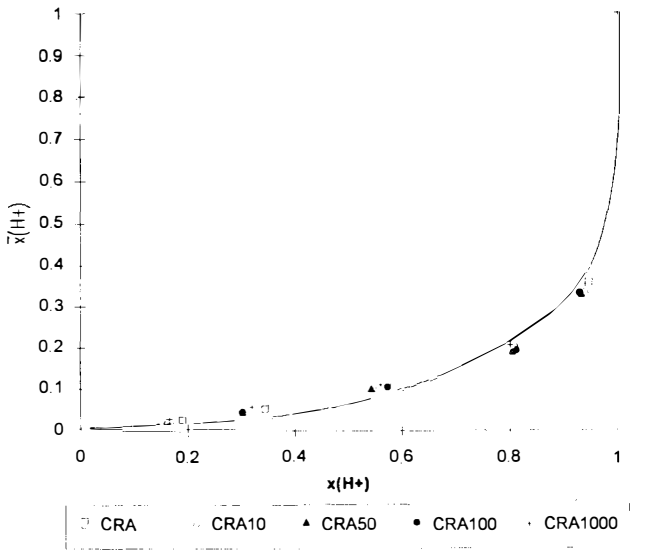

Fig. 4. Ion exchange isotherms: $HCl + CaCl_2$ solution.

3.5. Thickness of the unstirred layer

When an ion crossing a homogeneous membrane passes directly from the aqueous solution to the membrane phase, the thickness δ of the unstirred layer can be deduced from the value of the self-diffusion flux J_0 using the Helfferich equation [15]:

$$\frac{1}{J_0} = \frac{d}{\overline{Dc}} + \frac{2\delta}{Dc} \tag{1}$$

where D and c are the diffusion coefficient and the concentration respectively (bars indicate the membrane) and d is the membrane thickness. The thickness δ of the unstirred layer was determined with ^{22}Na-labelled NaCl solutions of concentrations ranging from 0.02 to 0.4 M. Plots $1/J^0_{Na}$ versus the reciprocal of the NaCl concentration for the CRA, CRA-5 and CRA-1000 membranes were straight lines whose slopes gave the value of δ. For a self-diffusion coefficient of Na^+ given by $D^{\bullet}_{Na} = 1.32 \times 10^{-5}$ cm^2 s^{-1} [16], the values of δ were 70 μm, 100 μm and 500 μm for the CRA, CRA-5 and CRA-1000 membranes respectively.

The second method for the determination of δ is based on the value of the limiting current density j_{lim} given by the classical relation for a 1 : 1 electrolyte:

$$j_{lim} = F\frac{Dc}{\delta(\bar{t}_i - t_i)} \tag{2}$$

where c is the electrolyte concentration, and $\bar{t}_i$ and t_i are the transport numbers of the counter-ion through the membrane and in the solution respectively. With $\bar{t}_{Na^+} = 1$ and $t_{Na^+} = 0.385$ in 0.1 M NaCl solution, we obtain $\delta = 70$ μm for the three membranes with an estimated discrepancy of 5 μm in δ. This value of δ is very close to that calculated for the non-modified CRA membrane. As expected, the Helfferich equation (1) is valid only when there is no resistance to the diffusion of ions at the membrane|solution interface.

3.6. Transport numbers of ions

The transport of an ion i is defined by

$$t_i = z_i J_i F / j \tag{3}$$

where z_i is the valency of ion i, J_i/mol cm^{-2} s^{-1} is its unidirectional flux, j/mA cm^{-2} is the applied current density and F is the Faraday constant.

For both the non-modified and modified CRA membranes, the fluxes of the co-ions (Cl^- for the $CaCl_2 + HCl$ mixed solutions and SO_4^{2-} for the $NiSO_4 + H_2SO_4$ mixed solutions) were always lower than 1%. Therefore the current must be transported by the

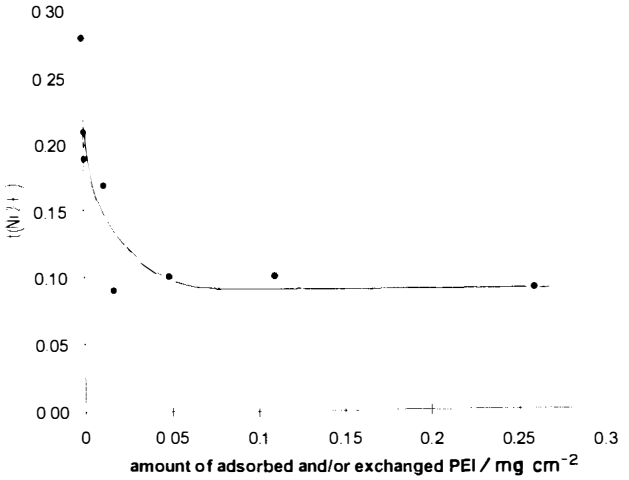

Fig. 5. Transport number $t_{Ni^{2+}}$ of the nickel ion vs. amount of adsorbed PEI.

counter-ions only. For the 0.5 M H_2SO_4 + 0.5 M $NiSO_4$ solution, the transport number $t_{Ni^{2+}}$ of the nickel cation is plotted versus the amount of PEI adsorbed on and/or ion-exchanged with the membrane in Fig. 5; $t_{Ni^{2+}}$ decreases abruptly as the amount of PEI adsorbed increases from 0 to 0.02 mg cm^{-2} and attains a constant value of about 0.10.

For the $CaCl_2$ + HCl solutions, the determination of the unidirectional fluxes of Ca^{2+} was achieved with current densities lower than the limiting values. Values of J_{H^+} were deduced from those of $J_{Ca^{2+}}$ using the equation

$$j = (2J_{Ca^{2+}} + J_{H^+})F \quad (4)$$

The unidirectional fluxes of Ca^{2+} obtained using the radiotracer technique were measured for the CRA, CRA-5 and CRA-1000 membranes, for three compositions of the electrolyte solution: ($\frac{1}{2}CaCl_2$ + HCl: 0.075 + 0.025, 0.05 + 0.05 and 0.025 + 0.075 mol l^{-1}) and for five current densities j (5, 10, 15, 20 and 30 mA cm^{-2}). The experimental results are collected in Table 1. An example of the increase in the selectivity of the modified membranes is illustrated in Fig. 6, where the unidirectional flux of calcium ion is plotted versus the value of the current density for a $\frac{1}{2}CaCl_2$ + HCl solution of 0.05 + 0.05 mol l^{-1}.

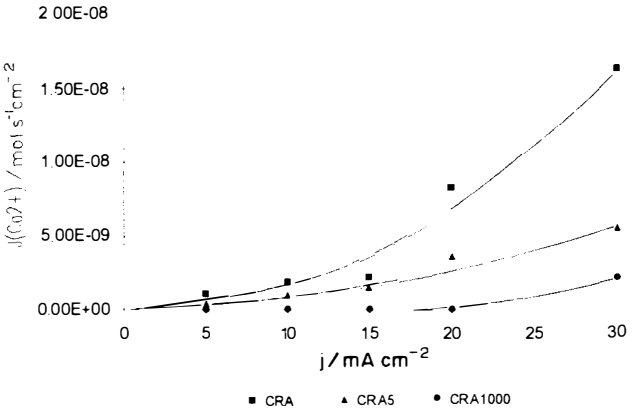

Fig. 6. Calcium flux vs. current density: HCl + $\frac{1}{2}CaCl_2$, 0.05 + 0.05 mol unit charge l^{-1}.

4. Discussion

4.1. Electrical resistance

As seen earlier, the PEI film increases the electrical resistance of modified membranes. This increase can

Table 1
Values of the electrotransport fluxes of Ca^{2+} and H^+ at different current densities in CRA, CRA-5 and CR-1000 membranes

j/mA cm^{-2}	CRA		CRA-5		CRA-1000 membrane	
	$10^9 J_{Ca^{2+}}$/ mol s^{-1} cm^{-2}	$10^8 J_{H^+}$/ mol s^{-1} cm^{-2}	$10^9 J_{Ca^{2+}}$/ mol s^{-1} cm^{-2}	$10^8 J_{H^+}$/ mol s^{-1} cm^{-2}	$10^{10} J_{Ca^{2+}}$/ mol s^{-1} cm^{-2}	$10^8 J_{H^+}$/ mol s^{-1} cm^{-2}
$\frac{1}{2}CaCl_2$ + HCl = 0.025 + 0.075 mol l^{-1}						
5	0.836	5.01	0.144	5.15	0	5.18
10	1.19	10.1	0.324	10.3	0	10.4
15	1.50	15.2	0.502	15.4	0	15.5
20	1.69	20.4	0.718	20.6	0.195	20.7
30	2.08	30.7	1.20	30.8	5.78	31.0
$\frac{1}{2}CaCl_2$ + HCl = 0.05 + 0.05 mol l^{-1}						
5	1.11	4.96	0.374	5.11	0	5.18
10	1.84	9.99	0.961	10.2	0	10.4
15	2.14	15.1	1.45	15.3	0	15.5
20	8.31	19.1	3.60	20.0	0.823	20.7
30	16.4	27.8	5.55	30.0	22.2	30.6
$\frac{1}{2}CaCl_2$ + HCl = 0.075 + 0.025 mol l^{-1}						
5	8.78	3.42	2.42	4.70	0	5.18
10	14.0	7.56	6.95	8.97	0.572	10.4
20	23.1	16.1	10.2	18.7	10.6	20.5
30	29.9	25.1	20.7	26.9	65.1	29.8

be ascribed to the entrance of low molar mass PEI molecules into the membrane [17]. Another possible explanation of the increase in the electrical resistance of the membrane is the creation of neutral zones at the membrane|PEI film interface corresponding to the electrostatic bonds between the amino groups of PEI and the sulphonic acid groups of the membrane [4,18,19]. This would mean that, above a PEI concentration of 100 ppm in the immersion solution, the number of ionic bonds between amino groups of PEI and sulphonic acid groups would be constant.

4.2. Ion-exchange isotherms and separation factors

As can be seen in Fig. 4, the exchange sites of the CRA and modified CRA membranes are preferentially balanced by divalent cations regardless of the proton content of the equilibrating solution. For the H^+–Ca^{2+} exchange represented by the relation.

$$2H^+ + \overline{Ca^{2+}} \Leftrightarrow 2\overline{H^+} + Ca^{2+} \qquad (5)$$

where bars refer to the membrane phase, the separation factor K is defined as

$$K = \frac{\bar{x}_{Ca^{2+}} x_{H^+}}{\bar{x}_{H^+} x_{Ca^{2+}}} \qquad (6)$$

where x_i is the equivalent ionic fraction of ion i [15]. As found for commercial cation-exchange membranes [11], for all the membranes studied the separation factor K is greater than unity and increases with the equivalent ionic fraction of the monovalent cation in the solution (Fig. 7). The easier entrance of divalent cations into the membrane could be explained by electrostatic interactions between counter-ions and fixed ion-exchange sites inside the membrane [11]. The presence of an anion-exchange film on the surface of the modified cation-exchange membranes does not affect this trend since all the curves in Fig. 7 merge.

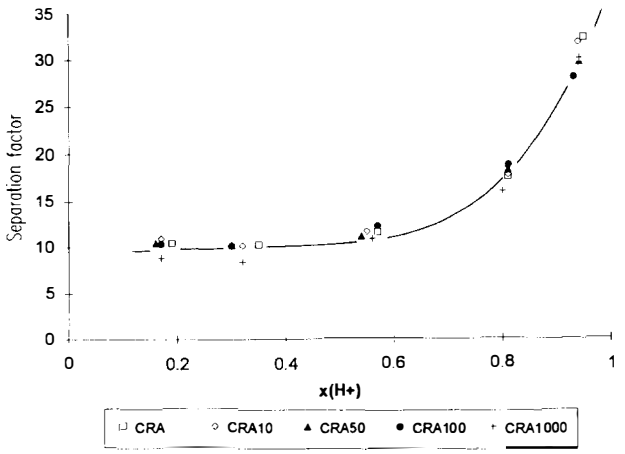

Fig. 7. Separation factor K vs. molar fraction of proton in the $HCl + CaCl_2$ electrolyte.

4.3. Preferential selectivity towards protons

As shown in Fig. 5, the PEI film on the surface of the membrane causes a decrease in the transport number of the nickel cation from 0.28 to 0.10 when the nickel cation is in competition with a proton. Indeed, it has been reported that about 90% of amino groups of the adsorbed or ion-exchanged PEI are not bonded with sulphonic groups of the membrane [13]. Therefore, in an acid solution, the PEI amino groups which are not fixed on the surface of the membrane are positively charged and form a repulsive barrier to the entrance of divalent cations into the membrane. Furthermore, proton transport could be facilitated by the PEI amino groups. In fact, as the amino groups are proton acceptors, the proton would move by hopping from one amino group to another on entering the membrane.

The increase in the selectivity of the modified membranes towards monovalent cations can be shown by a study of the transport numbers of counter-ions as well as by calculating the apparent rate constant of the interfacial transfer at the membrane|solution interface [11,20]. This part of the discussion deals with these two aspects.

4.4. Increase of the permselectivity towards monovalent cations

The transport numbers $t_{Ca^{2+}}$ of Ca^{2+} ions were calculated from the value of the unidirectional diffusion flux of calcium $J_{Ca^{2+}}$ using the relation

$$t_{Ca^{2+}} = 2FJ_{Ca^{2+}}/j \qquad (7)$$

In order to take into account the variation of this transport number with the composition of the equilibrating solution, a relative transport number $T_{H^+}^{Ca^{2+}}$ is defined:

$$T_{H^+}^{Ca^{2+}} = \frac{t_{Ca^{2+}}}{t_{H^+}} \frac{c_{H^+}}{c_{Ca^{2+}}} \qquad (8)$$

The variation of $T_{H^+}^{Ca^{2+}}$ with current density is shown in Figs. 8(a) and 8(b) for the CRA and the CRA-1000 membranes respectively. Comparison of these two sets of curves clearly shows the increase in selectivity towards the proton. Moreover, for the modified CRA-1000 membrane a total selectivity is observed for the composition $\frac{1}{2}CaCl_2 + HCl = 0.05 + 0.05$ mol l^{-1} and for a current density below 20 mA cm^{-2}. For this composition of the equilibrating solution, the electrical resistance increases from 2.1 to 4.1 Ω cm^2 while the relative transport number decreases from 0.08 to zero

and from 0.104 to 0.012 for applied current densities of 20 mA cm^{-2} and 30 mA cm^{-2} respectively.

4.5. Kinetics of ion transfer at the membrane | solution interface

When an ion-exchange membrane is exposed to an electrical field, both the interfacial electrochemical polarization and the kinetics of the ion transfers at the membrane | solution interface must be taken into account. The irreversibility of the ionic transfer is established when the value of the unidirectional flux is very different from that of self-diffusion [20]. The difference between the kinetics of the entrance of ions into a membrane can be determined from their individual apparent rate constants k on the basis of the Butler–Volmer equations. These equations were proposed for ion transfer through the interface between two non-miscible solutions [21] and can be applied to an interface between a solution and an ion-exchange membrane regardless of whether the latter is liquid or polymeric. The apparent rate constants $k_{Ca^{2+}}$ and k_{H^+} for the $Ca^{2+} + H^+$ system are deduced from [11,20].

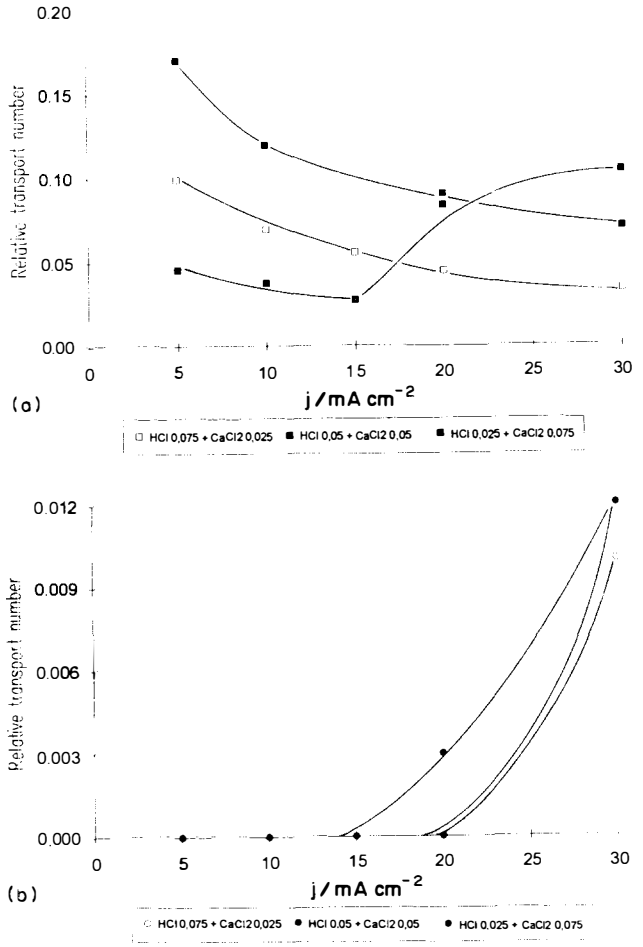

Fig. 8. Relative transport number $T_{H^+}^{Ca^{2+}}$ vs. current density: (a) non-modified CRA membrane; (b) modified CRA-1000 membrane.

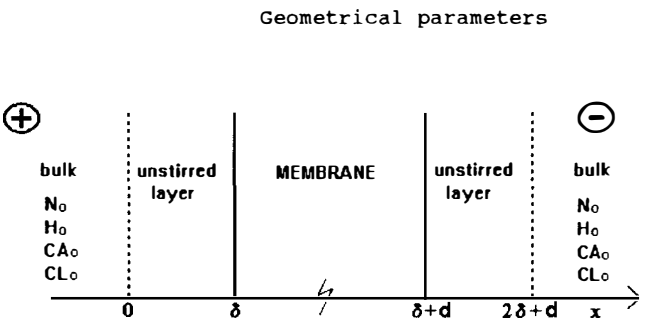

Fig. 9. Geometrical parameters and zones of the membrane | solution system.

$$J_{Ca^{2+}} = k_{Ca^{2+}} c^{w}_{Ca^{2+}} \quad (9a)$$

$$J_{H^+} = k_{H^+} c^{w}_{H^+} \quad (9b)$$

where $c^{w}_{Ca^{2+}}$ and $c^{w}_{H^+}$ are the concentrations of calcium ions and protons at the extreme end of the unstirred layer corresponding to $x = \delta$ (Fig. 9). The values of the apparent rate constants $k_{Ca^{2+}}$ and k_{H^+} can be obtained both from the experimental values of the unidirectional fluxes $J_{Ca^{2+}}$ and J_{H^+} and from the calculated values of the ionic concentrations at the extreme end of the anodic unstirred layer.

Determination of the concentration profiles within the anodic unstirred layer

Transport processes in the membranes are complex mainly because of the large coupling between ionic fluxes and between ion and solvent fluxes, e.g. electro-osmosis [22,23]. For an easier resolution of the transport equations, the membrane was placed between two identical solutions of equal concentrations of a total of 0.1 mol of unit charge. Moreover, the volumes of the external solutions are sufficiently large that concentration changes due to ion transport remain negligible. From this last condition, it can be assumed that steady state transport is attained and the electro-osmotic flux of solvent is minimized. In addition, the applied current density was always lower than the limiting value in order to avoid flux of H^+ and OH^- ions resulting from water-splitting at the membrane | solution interface.

Under these conditions, the ion transport can be described by the Nernst–Planck electrodiffusion equations at the membrane | solution interface. For the HCl + $CaCl_2$ system, we obtain

$$J_{H^+} = -D_{H^+}\left(\frac{dc_{H^+}}{dx} + \frac{c_{H^+} F}{RT}\frac{d\Phi}{dx}\right) \quad (10a)$$

$$J_{Ca^{2+}} = -D_{Ca^{2+}}\left(\frac{dc_{Ca^{2+}}}{dx} + 2\frac{c_{Ca^{2+}} F}{RT}\frac{d\Phi}{dx}\right) \quad (10b)$$

$$J_{Cl^-} = -D_{Cl^-}\left(\frac{dc_{Cl^-}}{dx} - \frac{c_{Cl^-} F}{RT}\frac{d\Phi}{dx}\right) \quad (10c)$$

The relation between the potential and the distribution of electrical charges is governed by the Poisson equation

$$\frac{d^2\Phi}{dx^2} = -\frac{\rho}{\varepsilon_0\varepsilon_r} \tag{11}$$

where ε_0 is the permittivity of vacuum, ε_r is the relative permittivity, Φ is the electrical potential and ρ is the local charge density which is defined as

$$\rho = (2c_{Ca^{2+}} + c_{H^+} - c_{Cl^-})F \tag{12}$$

The aqueous polarization layer is a medium with no fixed charge distribution.

In previous work, Eqs. (10)–(12) were solved by assuming electroneutrality within the unstirred layer [11]. From Eqs. (11) and (12) this assumption led to

$$\frac{d\Phi^2}{dx^2} = 0 \tag{13a}$$

or

$$\frac{\Phi_{(\delta)} - \Phi_{(0)}}{\delta} = \frac{\Delta\Phi}{\delta} = E \tag{13b}$$

and consequently

$$(2c_{Ca^{2+}} + c_{H^+} - c_{Cl^-}) = 0 \tag{14}$$

Eqs. (10a), (10b), (10c) and (14) were solved using an analytical method including dimensionless parameters.

Both non-modified and modified membranes were used in this study. Although all the experimental values were established for current densities lower than the limiting value, it was not obvious that the electroneutrality could be assumed throughout the whole thickness of the unstirred layer, especially in the close vicinity of the modified membrane surface. Consequently, the concentration and potential profiles have been calculated taking into consideration both the electrodiffusion equations and the Poisson equation. In this case, the system of equations (10a)–(10c) and (11), which is a non-linear boundary problem, was derived using a numerical method.

Reduced variables are defined to simplify the equations:

$$\xi = \frac{x}{\delta} \tag{15a}$$

$$\phi = F\frac{\Phi}{RT} \tag{15b}$$

$$\sigma = F\frac{\varepsilon_0\varepsilon_r RT}{N_{(0)}F^2\delta^2} \tag{15c}$$

$$H = \frac{c_{H^+(x)}}{N_{(0)}} \tag{15d}$$

$$CA = 2\frac{c_{Ca^{2+}(x)}}{N_{(0)}} \tag{15e}$$

$$CL = \frac{c_{Cl^-(x)}}{N_{(0)}} \tag{15f}$$

$$u = \frac{J_{H^+}\delta}{D_{H^+}N_{(0)}} \tag{15g}$$

$$v = \frac{J_{Ca^{2+}}\delta}{D_{Ca^{2+}}N_{(0)}} \tag{15h}$$

$$w = \frac{J_{Cl^-}\delta}{D_{Cl^-}N_{(0)}} \tag{15i}$$

where $c_{H^+(x)}$, $c_{Ca^{2+}(x)}$ and $c_{Cl^-(x)}$ are the concentrations of proton, calcium and chloride ions, and $N_{(0)}$ is the concentration of the bulk solution expressed in moles of unit charge per litre. We have

$$N_{(0)} = c_{H^+} + 2c_{Ca^{2+}} = c_{Cl^-} \tag{16}$$

With the above transformations, the system of equations (10a)–(10c), (11) and (12) becomes

$$H + CA - CL + \sigma\frac{d^2\phi}{d\xi^2} = 0 \tag{17a}$$

$$\frac{dCL}{d\xi} - CL\frac{d\phi}{d\xi} = 0 \tag{17b}$$

$$\frac{1}{2}\frac{dCA}{d\xi} + CA\frac{d\phi}{d\xi} + v = 0 \tag{17c}$$

$$\frac{dH}{d\xi} + H\frac{d\phi}{d\xi} + u = 0 \tag{17d}$$

where the unknown parameters are H, CA, CL and ϕ, and the boundary conditions are

$$H_{(\xi=0)} = H_0 \tag{18a}$$

$$CA_{(\xi=0)} = CA_0 \tag{18b}$$

$$CL_{(\xi=0)} = CL_0 \tag{18c}$$

$$\phi_{(\xi=0)} = 0 \tag{18d}$$

$$\phi_{(\xi=1)} = V \tag{18e}$$

V is the potential value obtained by assuming a constant electrical field within the unstirred layer. The numerical solution method is presented in the Appendix. The calculations were performed with the following parameter values [24]:

$D_{H^+} = 9.3 \times 10^{-5}$ cm^2 s^{-1}

$D_{Ca^{2+}} = 0.77 \times 10^{-5}$ cm^2 s^{-1}

$\delta = 70$ μm $\quad R = 8.314$ J mol^{-1} K^{-1}

$T = 294$ K $\quad F = 96500$ C mol^{-1}

$\varepsilon_0 = 8.854 \times 10^{-12}$ C V^{-1} cm^{-1} $\quad \varepsilon_r = 75.4$

The experimental values for J_{H^+} and $J_{Ca^{2+}}$ were taken from Table 1.

Both concentration and potential profiles have been calculated for CRA, CRA-5 and CRA-1000 membranes, for three compositions of the equilibrating solutions ($\frac{1}{2}CaCl_2$ + HCl: 0.075 + 0.025, 0.05 + 0.05 and 0.025 + 0.075 mol l^{-1}) and for four current densities j (5, 10, 20 and 30 mA cm^{-2}). Of all these results, we have chosen to present only those for two membranes (the non-modified CRA membrane and the modified CRA-1000 membrane) and one equilibrating solution composition (0.05 + 0.05 mol l^{-1}).

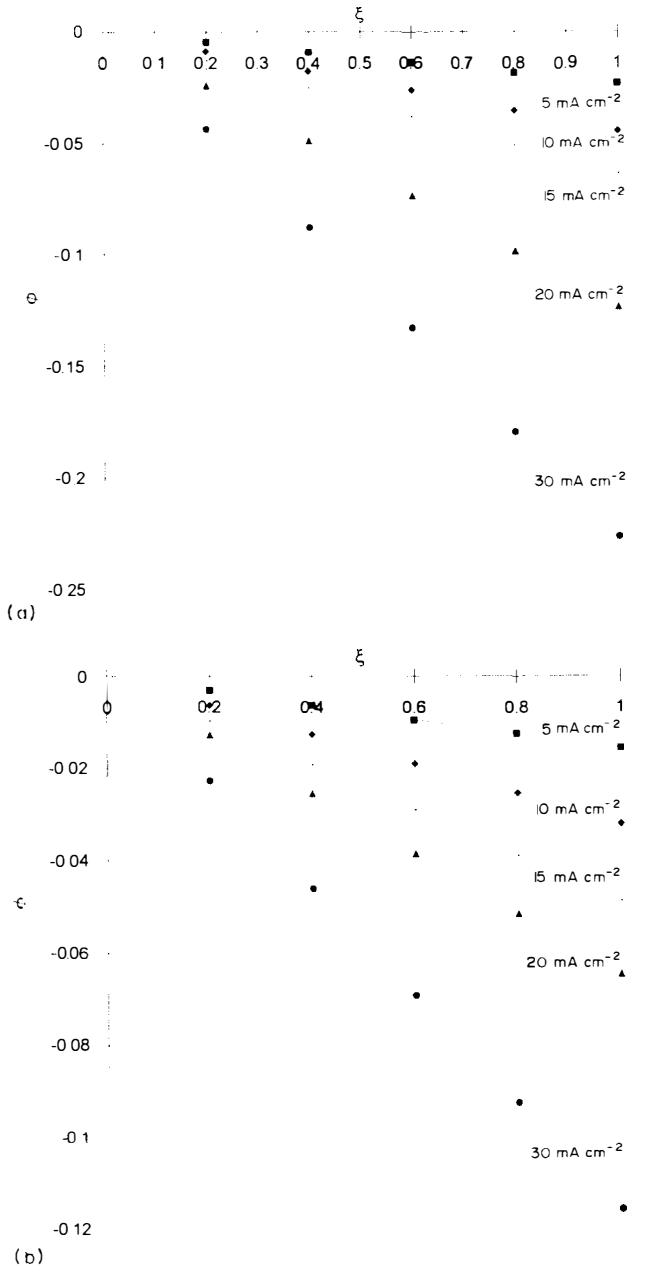

Fig. 10. Potential profiles within the unstirred layer of the anodic compartment: (a) non-modified CRA membrane; (b) modified CRA-1000 membrane. Solution: HCl + $\frac{1}{2}CaCl_2$, 0.05 + 0.05 mol unit charge l^{-1}. Symbols, concentrations calculated from the assumption of the constant electrical field (analytical resolution); dotted lines, concentrations calculated from the Nernst–Planck–Poisson equations (numerical resolution).

Table 2
Calculated values of the ratio of the apparent rate constants of the penetration of proton and calcium into the CRA, CRA-5 and CRA-100 membranes at different current densities

	$k_{H^+}/k_{Ca^{2+}}$			
	5 mA cm^{-2}	10 mA cm^{-2}	20 mA cm^{-2}	30 mA cm^{-2}
HCl + $\frac{1}{2}CaCl_2$ = 0.025 + 0.075 mol l^{-1}				
CRA	6.0	8.6	14.6	33.9
CRA-5	34	25	62	93
CRA-1000	> 10000	4130	1000	385
HCl + $\frac{1}{2}CaCl_2$ = 0.05 + 0.05 mol l^{-1}				
CRA	26	33	14	10.9
CRA-5	73	60	39	56
CRA-1000	> 10000	> 10000	1970	165
HCl + $\frac{1}{2}CaCl_2$ = 0.075 + 0.025 mol l^{-1}				
CRA	10.0	15.8	27.7	43.3
CRA-5	60	60	71	84
CRA-1000	> 10000	> 10000	2840	183

The potential profiles ϕ are shown in Figs. 10(a) and 10(b) for the CRA and CRA-1000 membranes respectively. The dotted lines correspond to the values obtained from numerical resolution, while the symbols correspond to the values obtained from the analytical resolution method assuming a constant electrical field. The two sets of values are very similar under applied current conditions lower than the limiting values.

The plots of concentration profiles are given in Figs. 11(a) and 11(b) for the CRA and CRA-1000 membranes respectively.

Apparent rate constant of the penetration of ions

The values of the concentrations for $x = \delta$ are used for the calculations of the apparent rate constants $k_{Ca^{2+}}$ and k_{H^+}. It can be seen that in the binary system HCl + $\frac{1}{2}CaCl_2$ = 0.05 + 0.05 mol l^{-1} (Fig. 11(b)) there is an accumulation of Ca^{2+} in the polarization layer and, of course, a depletion of protons.

The calculated values of the ratio of the apparent rate constants of the penetration of proton and calcium ions into the non-modified CRA membrane and the modified CRA-1000 membrane are reported in Table 2 for different values of the composition of the external solution. For the CRA-1000 membrane with applied current densities below 20 mA cm^{-2}, the proton–calcium separation is excellent.

5. Conclusion

This work shows that the origin of the active mechanism of the adsorbed PEI layer is kinetic and not

thermodynamic. The equilibrium exchange isotherm is not affected by surface modification, while the apparent rate constant of the entry step of Ca^{2+} into the membrane is substantially changed. The ratio of the apparent rate constants of proton with respect to the divalent cation is increased. To obtain the values of these apparent rate constants, it has been necessary to derive the Nernst–Planck–Poisson equation system in the polarization layer. In some cases, the current transport through the modified membranes produces an accumulation of divalent ions on the aqueous side of the membrane|solution interface.

Appendix. The numerical algorithm

Partial resolution

The equations of the problem in the interval]0,1[are

$$-\delta\frac{d^2\phi}{d\xi^2} + CL - H - CA = 0 \qquad (A1)$$

$$\frac{dCL}{d\xi} - CL\frac{d\phi}{d\xi} = 0 \qquad (A2)$$

$$\frac{1}{2}\frac{dCA}{d\xi} + CA\frac{d\phi}{d\xi} + v = 0 \qquad (A3)$$

$$\frac{dH}{d\xi} + H\frac{d\phi}{d\xi} + u = 0 \qquad (A4)$$

where the coefficients σ, v and u are given. The boundary conditions are

$$\phi(0) = 0 \quad \text{and} \quad \phi(1) = -V \qquad (A5)$$

$$CL(0) = CL_0 \qquad (A6)$$

$$CA(0) = CA_0 \qquad (A7)$$

$$H(0) = H_0 \qquad (A8)$$

where V, CL_0, CA_0 and H_0 are given. From Eq. (A2)

$$CL = CL(0)\exp(\phi) = CL_0\exp(\phi) \qquad (A9)$$

Equations (A3) and (A4) become

$$CA = c_1\exp(-2\phi) \quad \text{with} \quad \frac{dc_1}{d\xi} = -2v\exp(2\phi) \qquad (A10)$$

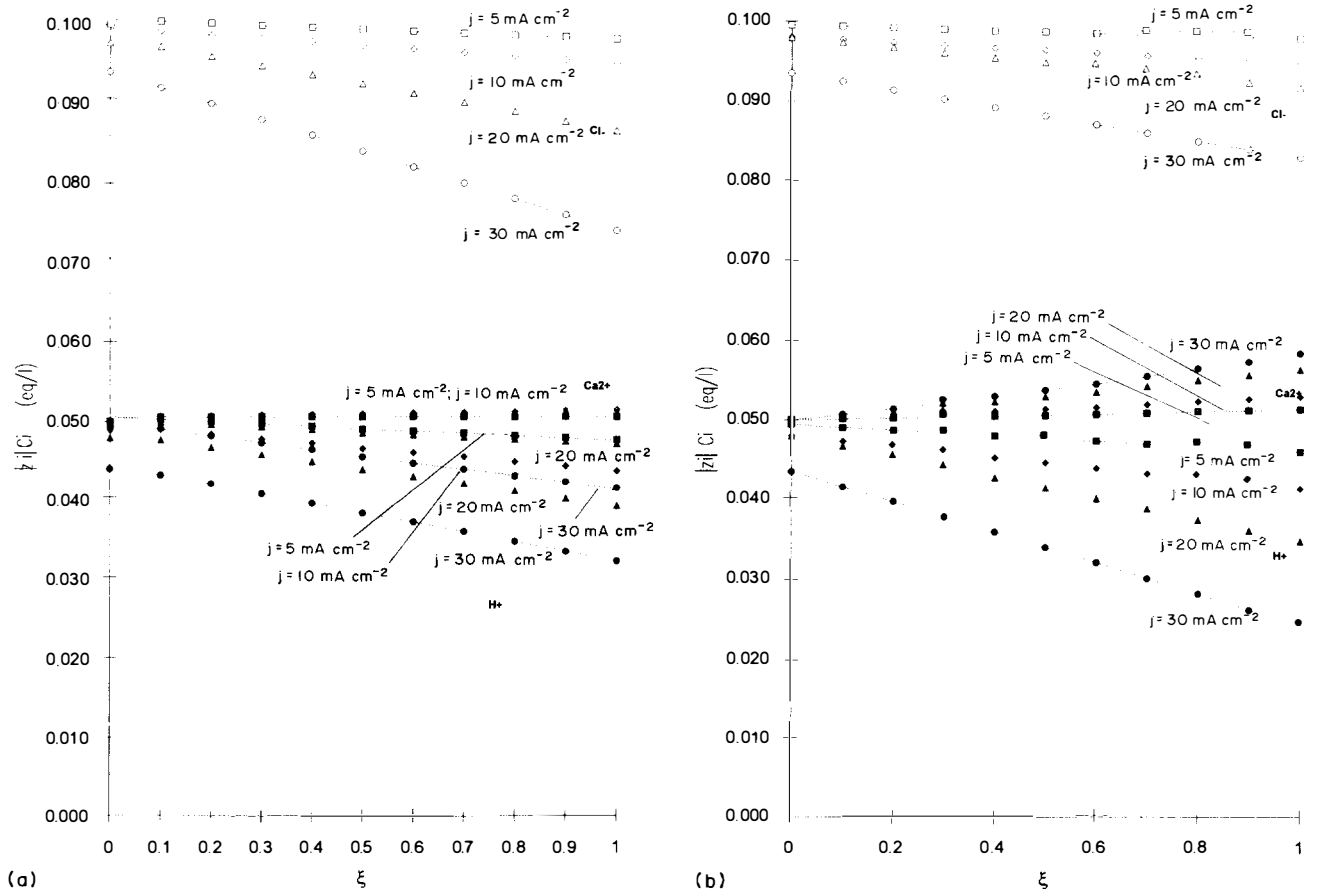

Fig. 11. Concentration profiles within the unstirred layer of the anodic compartment: (a) non-modified CRA membrane; (b) modified CRA-1000 membrane. Solution: HCl + $\frac{1}{2}CaCl_2$, 0.05 + 0.05 mol unit charge l^{-1}. Symbols, concentrations calculated from the assumption of the constant electrical field (analytical resolution); dotted lines, concentrations calculated from the Nernst–Planck–Poisson equations (numerical resolution).

$$H = c_2 \exp(-\phi) \quad \text{with} \quad \frac{dc_2}{d\xi} = -u \exp(\phi) \qquad (A11)$$

Therefore the differential system (A1)–(A4) can be written

$$-\sigma \frac{d^2\phi}{d\xi^2} + CL_0 \exp(\phi) - c_1 \exp(-2\phi) - c_2 \exp(-\phi) = 0 \qquad (A12)$$

$$\frac{dc_1}{d\xi} + 2v \exp(2\phi) = 0 \qquad (A13)$$

$$\frac{dc_2}{d\xi} + u \exp(\phi) = 0 \qquad (A14)$$

The finite-difference method

Eqs. (A12)–(A14) are discretized using a second-order finite-difference scheme. The interval]0,1[is decomposed in subintervals of step h. We define the nodes $\xi_i = ih$ for $i = 0, N+1$, with $\xi_0 = 0$ and $\xi_{N+1} = 1$. Eq. (12) becomes

$$-\sigma \frac{\phi(\xi_{i+1}) - 2\phi(\xi_i) + \phi(\xi_{i-1})}{h^2} + CL_0 \exp[\phi(\xi_i)] - c_1(\xi_i) \exp[-2\phi(\xi_i)] - c_2(\xi_i) \exp[-\phi(\xi_i)] = 0$$
$$1 \leqslant i \leqslant N \qquad (A15)$$

We define

$$\phi(\xi_i) = \phi_i \qquad 0 \leq i \leq N+1 \qquad (A16)$$

$$c_1(\xi_i) = c_{1i} \qquad 0 \leq i \leq N+1 \qquad (A17)$$

$$c_2(\xi_i) = c_{2i} \qquad 0 \leq i \leq N+1 \qquad (A18)$$

Eq. (A15) is written

$$-\sigma \frac{\phi_{i+1} - 2\phi_i + \phi_{i-1}}{h^2} + CL_0 \exp(\phi_i) - c_{1i} \exp(-2\phi_i) - c_{2i} \exp(-\phi_i) = 0$$
$$\text{for } 1 \leq i \leq N \qquad (A19)$$

with

$$\phi_0 = \phi(0) = 0 \quad \text{and} \quad \phi_{N+1} = \phi(1) = -V \qquad (A20)$$

Eqs. (A13) and (A14) are solved using an implicit Euler scheme:

$$\frac{c_{1i+1} - c_{1i}}{h} = -2v \exp(2\phi_{i+1})$$

or

$$c_{1i+1} = c_{1i} - 2hv \exp(2\phi_{i+1}) \qquad (A21)$$

$$\frac{c_{2i+1} - c_{2i}}{h} = -u \exp(\phi_{i+1})$$

or

$$c_{2i+1} = c_{2i} - hv \exp(\phi_{i+1}) \qquad (A22)$$

for $1 \leq i \leq N+1$. Eq. (A21) becomes

$$c_{1i} = c_{10} - 2hv \sum_{j=1}^{j=i} \exp(2\phi_j) \qquad (A23)$$

and then

$$c_{1i} = CA_0 - 2hv \sum_{j=1}^{j=i} \exp(2\phi_j) \qquad (A24)$$

Likewise, Eq. (A22) becomes

$$c_{2i} = H_0 - hu \sum_{j=1}^{j=i} \exp(\phi_j) \qquad (A25)$$

Eqs. (A23) and (A25) are now introduced in Eq. (A19) which becomes

$$-\sigma \frac{\phi_{i+1} - 2\phi_i + \phi_{i-1}}{h^2} + CL_0 \exp(\phi_i) - \left(CA_0 - 2hv \sum_{j=1}^{j=i} \exp(2\phi_j)\right) \exp(-2\phi_i) - \left[H_0 - hu \sum_{j=1}^{j=i} \exp(\phi_j)\right] \exp(-\phi_i) = 0$$
$$\text{for } 1 \leq i \leq N \qquad (A26)$$

A non-linear system of order N is obtained:

$$F(\phi) = 0 \qquad (A27)$$

with

$$\phi = (\phi_1, \phi_2, \ldots, \phi_N) \qquad (A28)$$

Tangent matrix computation

Standard Newton's method is used in order to solve the system (A27). At iteration k, the vector ϕ^k is computed using the following algorithm (ϕ^0 is a given vector):

$$\nabla F(\phi^{k-1})(\phi^k - \phi^{k-1}) = -F(\phi^{k-1}) \qquad (A29)$$

where ∇F is the Jacobian of F (the tangent matrix).

The main difficulty is the computation of this matrix. This is a lower Hessenberg matrix (a lower triangular matrix with an upper diagonal). If we denote the terms of the tangent matrix by a_{ij}, then for $1 \leq i, j \leq N$

$$a_{ii+1} = -\frac{\sigma}{h^2} \qquad \text{for } 1 \leq i \leq N \qquad (A30)$$

$$a_{ii} = \frac{2\sigma}{h^2} + CL_0 \exp(\phi_i) + 2\left[CA_0 - 2hv \sum_{j=1}^{j=i-1} \exp(2\phi_j)\right] \exp(-2\phi_i) + \left[H_0 - hu \sum_{j=1}^{j=i-1} \exp(\phi_j)\right] \exp(-\phi_i)$$
$$\text{for } 1 \leq i \leq N \qquad (A31)$$

$$a_{i-1i} = -\frac{\sigma}{h^2} + 4hv\ \exp(2\phi_{i-1})\ \exp(-2\phi_i) + hu\ \exp(\phi_{i-1})\ \exp(-\phi_i) \qquad \text{for } 1 \le i \le N \tag{A32}$$

$$a_{ji} = 4hv\ \exp(2\phi_j)\ \exp(-2\phi_i) + hu\ \exp(\phi_j)\ \exp(-\phi_i)$$
$$\text{for } 1 \le i \le N \text{ and } 1 \le j \le i-2 \tag{A33}$$

The linear system

The linear system (A29) is solved using an ascendant Gauss method. The system (A29) is easily transformed in a lower triangular system. The system obtained is solved using a single descent. The second member of Eq. (A29) is denoted b and the solution is denoted x. The algorithm is written as follows.

First step (ascendant part):

$$b_{k-1} = b_{k-1} - \frac{a_{k-1k}b_k}{a_{kk}} \qquad \text{for } k = N,\ 1 \text{ step } -1 \tag{A34}$$

$$a_{ij} = a_{ij} - \frac{a_{k-1k}a_{kj}}{a_{kk}} \quad \text{for } j = k-1,\ N-1 \tag{A35}$$

Second step (descent step):

$$x_1 = \frac{b_1}{a_{11}} \tag{A36}$$

$$x_j = \frac{x_j - \sum_{k=1}^{k=j-1} a_{ik}x_k}{a_{jj}} \qquad \text{for } j = 2,\ N \tag{A37}$$

Concluding remarks

The number of operations at each Newton iteration is $(7/2)N^2 + (9/2)N$. A classical solution of the Eq. (A29) has a number of operations equal to $(2/3)N^3$. The number of operations for a standard finite-difference scheme applied to the initial equations (A1)–(A4) is $(2/3)(4N-3)^3$. For example, for $N = 31$, 1 370 000 operations are required in the classical case and 3503 for the present algorithm.

Ten Newton iterations are usually required for this problem. Convergence is assumed if the functions of the problem (ϕ, CA, CL and H) are bounded. This convergence is not quadratic, as for classical problems, but only linear.

Nomenclature

c	concentration, mol m^{-3}
d	membrane thickness, m
D_i	diffusion coefficient of species i, m^2 s^{-1}
E	electrical field, V m^{-1}
F	Faraday constant
j	current density, A m^{-2}
j_{lim}	limiting current density, A m^{-2}
J_0, $J_{Ca^{2+}}$, J_{H^+}	self-diffusion and unidirectional fluxes, mol m^{-2} s^{-1}
$k_{Ca^{2+}}$, k_{H^+}	apparent rate constants of calcium and proton, m s^{-1}
K	separation factor
$N_{(0)}$	concentration of the bulk solution expressed in moles of unit charge per litre
R	gas constant (8.314 J mol^{-1} K^{-1})
t_i	transport number of species i
T	temperature, K
$T_{H^+}^{Ca^{2+}}$	relative transport number of calcium with respect to proton
x	abscissa
x_i	equivalent ionic fraction of species i
z	valency
δ	thickness of the unstirred layer
ε_0	permittivity of vacuum
ε_r	relative permittivity, F m^{-1}
Φ	electrical potential, V
ρ	charge density, C m^{-3}

Reduced variables

H, CA, CL reduced concentrations for proton, calcium and chloride respectively

$$\xi = x/\delta$$
$$\phi = F(\Phi/RT)$$
$$\sigma = F\left(\varepsilon_0\varepsilon_r RT/N_{(0)}F^2\delta^2\right)$$
$$u = J_{H^+}\delta/D_{H^+}N_{(0)}$$
$$v = \frac{J_{Ca^{2+}}\delta}{D_{Ca^{2+}}N_{(0)}}$$
$$w = \frac{J_{Cl^-}\delta}{D_{Cl^-}N_{(0)}}$$

References

[1] T. Sata, R. Izuo, Y. Mizutani and R. Yamane, J. Colloid Interface Sci., 40 (3) (1972) 317.
[2] Y. Tanaka and M. Seno, J. Membr. Sci., 8 (1981) 115.
[3] T. Sata, J. Colloid Interface Sci., 44 (3) (1973) 393.
[4] Y. Mizutani, J. Membr. Sci., 54 (1990) 233.
[5] Z. Ogumi, Y. Uchimoto, M. Tsujikaw, K. Yasuda and Z. Takehara, J. Mebr. Sci., 54 (1990) 163.
[6] H. Ohya, M. Kuromoto, H. Matsumoto, K. Matsumoto and Y. Negishi, J. Membr. Sci., 51 (1990) 201.
[7] C. Gavach, J.L. Bribes, A. Chapotot, J. Maillols, G. Pourcelly, J. Sandeaux, R. Sandeaux and I. Tugas, J. Phys. (Paris), Colloq. C1, 4 (1994) C1-233.

[8] Y. Tanaka and M. Seno, J. Membr. Sci., 8 (1981) 115.
[9] T. Sata and R. Izuo, J. Membr. Sci., 45 (1989) 209.
[10] T. Sata, J. Polym. Sci. Polym. Chem. Ed., 16 (1978) 1063.
[11] A. Chapotot, G. Pourcelly and C. Gavach, J. Membr. Sci., 96 (1994) 167.
[12] A. Lindheimer, J. Molénat and C. Gavach, J. Electroanal. Chem., 216 (1987) 71.
[13] M. Taky, G. Pourcelly, F. Lebon and C. Gavach, J. Electroanal. Chem., 336 (1992) 171.
[14] C. Gavach, A. Lindheimer, D. Cros and B. Brun, J. Electroanal. Chem., 33 (1985) 190.
[15] F. Helfferich, Ion Exchange, McGraw-Hill, New York, 1962.
[16] R. Parsons (Ed.), Handbook of Electrochemical Constants, Butterworths, London, 1959.
[17] T. Sata, Colloid & Polym. Sci., 256 (1978) 62.
[18] T. Sata and R. Izuo, Colloid Polym. Sci., 256 (1978) 757.
[19] T. Sata, Kolloid-Z., Z. Polym., 250 (1972) 980.
[20] G. Pourcelly, I. Tugas and C. Gavach, J. Membr. Sci., 85 (1993) 195.
[21] C. Gavach, B. D'Epenoux and F. Henry, J. Electroanal. Chem., 64 (1975) 107.
[22] I.C. Bassignana and H. Reiss, J. Phys. Chem., 87 (1983) 136.
[23] C. Selvey and H. Reiss, J. Membr. Sci., 30 (1987) 75.
[24] B.E. Conway in Electrochemical Data, Elsevier, London, 1952.